Stipica Novoselac[1], Dražan Kozak[1], Todor Ergić[1], Ivan Šimić[2]

INFLUENCE OF STRESS GRADIENTS ON BOLTED JOINT FATIGUE BEHAVIOUR UNDER DIFFERENT PRELOADS AND CYCLIC LOADS RATIO

UTICAJ GRADIJENATA NAPONA NA ZAMOR VIJČANE VEZE POD DEJSTVOM RAZLIČITIH PREDOPTEREĆENJA I ODNOSA CIKLIČNIH OPTEREĆENJA

Originalni naučni rad / Original scientific paper
UDK /UDC: 621.882:539.3/.4
Rad primljen / Paper received: 21.02.2014.

Adresa autora / Author's address:
[1)] Josip Juraj Strossmayer University of Osijek, Mechanical Engineering Faculty in Slavonski Brod, Croatia,
E-mail: dkozak@sfsb.hr
[2)] University of Zagreb, Faculty of Mechanical Engineering and Naval Architecture, Croatia

Keywords
- threaded joint fatigue
- stress gradients
- multiaxial fatigue

Ključne reči
- zamor vijčanog spoja
- gradijenti napona
- višeosni zamor

Abstract

Threaded joints have sharp notches which generate a localized multiaxial stress field with high stress gradients. Fatigue strength of mechanical structures is a nonlocal phenomenon, and spatial distribution of stresses influence fatigue behaviour, not only the local value of stress. Therefore, the stress gradient approach is used for the assessment of fatigue behaviour due to high stress concentration and stress gradients. In order to predict the multiaxial highcycle fatigue, the stress based critical plane approach combined with Rainflow cycle counting and damage accumulation to estimate a multiaxial fatigue failure criterion are used. The stress gradients influence on the M10 bolt, strength class 10.9, highcycle fatigue are estimated with IABG, FemFat, Stieler and FKM-Guideline methods. Methods are compared mutually and with the results obtained without the influence of stress gradients. The fatigue endurance limit of a threaded joint at a very high survival probability is estimated with influence factors of size, surface roughness, stress gradients, statistics, mean stresses and mean stress rearrangements in case of local plastification with Neuber-hyperbola, and the Haigh diagram is modified with the stress gradient influence. A finite element model is created with nonlinear contact interactions between engaged threads and other parts. During the lifetime, the first load is due to the bolt tightening which is defined as 50, 70 and 90 % of the bolt material yield strength. Moreover, tensile eccentric forces with constant amplitudes are applied with a load ratio of 0.1, 0.5 and 0.9.

Izvod

Navojni spojevi sadrže oštre zareze koji stvaraju lokalno višeosno stanje napona s velikim gradijentima napona. Zamorna čvrstoća mehaničkih konstrukcija nije lokalni fenomen, a prostorna raspodela napona utiče na zamorno ponašanje, a ne samo lokalna vrednost napona. Zbog toga je pristup s gradijentima napona korišćen za određivanje zamornog ponašanja usled visokih koncentracija napona i gradijenata napona. Za predviđanje višeosnog visokocikličnog zamora, pristup teorije kritičnih ravni, utemeljen na naponima i u kombinaciji sa Rainflow metodom brojanja ciklusa i akumulacije oštećenja, korišćeni su za određivanje višeosnog zamornog kriterijuma. Uticaj gradijenata napona na Visokociklični zamor M10 vijka s klasom čvrstoće 10.9, procenjen je metodama IABG, FemFat, Stieler i FKM. Metode su upoređene i s rezultatima dobijenim bez uticaja gradijenata napona. Dinamička izdržljivost navojnog spoja pri vrlo visokoj verovatnoći preživljavanja određena je s uticajnim faktorima veličine, površinske hrapavosti, gradijenata napona, statistike, srednjih napona i sređivanja srednjih napona u slučaju lokalne plastifikacije s Nojberovom hiperbolom i modifikacijom Hejgovog dijagrama s uticajem gradijenata napona. Model konačnih elemenata izgrađen je s nelinearnim kontaktima između navoja u sprezi i drugih delova. Tokom životnog veka, prvo opterećenje je usled pritezanja vijka koje je definisano kao 50, 70 i 90% od granice tečenja materijala vijka. Nadalje, zatezne ekscentrične sile su primenjene s konstantnim amplitudama i odnosom opterećenja od 0,1, 0,5 i 0,9.

INTRODUCTION

The bolted joints fatigue behaviour is in fatigue problem areas and requires further research and development, /1/. It is noteworthy that also the fatigue of various structures still remains a practical problem /2/. Many types of dynamically loaded threaded joints subjected to large numbers of cycles where the fatigue failures are undesirable can be found in the automotive industry (connecting rods, cylinder head-crankcase joints, main bearing cap-crankcase joints, etc.), /3/, offshore and subsea industry (wellheads, x-mas trees, drilling risers, etc.), /4-6/, dental implants, and in many

other industries. Load distribution and stresses in threaded joints have been widely investigated, /7-24/. Results show that the load is not uniformly distributed along the threads and that the first engaged thread is subjected to the highest load. Due to unfavourable distribution, the first thread root results in very high stress concentration factor (K_t), which is usually $K_t \approx 4$–10, /25/. Fatigue analysis of threaded joints using the local strain approach was presented by Schneider et al. /26/. Lifetime prediction method for threaded joints was proposed on a drillstring joint used in the oil and gas industry /27/. The method was based on a finite element (FE) and a fatigue analysis using the Dang Van criterion. The comparisons with experimental results showed difficulties to estimate the fatigue life on structures due to high stress gradient and scale effects. A similar work has also been presented with bolt fatigue lifetime evaluation using Dang Van criterion, /28/. Recently, additional study of the stress gradient effect on fatigue has been performed using the Dang Van criterion, /29-30/. Fatigue studies have been performed on threaded joints but mostly on axially loaded bolts, /31/. Investigation of the eccentric cyclic loading effect on the fatigue life of bolts has been investigated and it was found that eccentric loading reduces the fatigue life of bolts by an amount proportional to the increase in the local stress amplitude produced by the eccentricity, /31/. Assessment of bolt failures has revealed that bending loads superimpose on the tensile loads. A recent review by Patterson, /32/, evaluated the different methods for bolt fatigue life prediction. Even if the loading in the threaded joint is uniaxial, multiaxial (triaxial) stress state exists at the thread roots. Fatigue of the bolted joints requires the use of a multiaxial fatigue criterion, /33/. The stress distribution in notched and unnotched specimens are entirely different, /2/. The damage evaluation without considering stress triaxiality results with unrealistic fracture, /34/. An additional complex feature of fatigue at notches is the notch size effect which leads to different fatigue strengths for notches with different dimensions but with the same K_t. This is also one additional reason to take stress gradients into account, /35/.

The critical plane approaches are based on applied cyclic strain, stress or energy components. A comprehensive overview of the multiaxial fatigue failure criteria based on critical plane approach with stress, strain and strain energy density criteria for fatigue damage was presented by Karolczuk and Macha, /36/. Although the importance of maximum shear plane is from early fatigue studies, it was not up until Findley /37/, who formulated it. He proposed the addition of alternating shear stress and normal stress component on the plane of maximum shear as the controlling parameter of fatigue. Forsyth /38/ defined fatigue crack growth as a two stage process, where stage I corresponds to Mode II crack growth (caused by shear component) and stage II corresponds to Mode I crack growth (induced by normal components). This justified the use of both shear and normal components in fatigue parameter definition, /39/. McDiarmid /40/ modified the Findley's stress-based model to consider different cracking responses. The state-of-the-art overview shows that the majority of approaches which estimate multiaxial fatigue behaviour in high-cycle fatigue (HCF) regime are either stress or energy quantities based on the critical plane approach, /41-46/. It is based on experimental investigations which show that in metallic materials fatigue cracks initiate and grow on certain planes, /47/. Critical plane approach takes as a starting point that the fatigue damage reaches its maximum value on the plane of maximal shear stress amplitude τ_A (the so-called critical plane) /48-52/, and it is based on the hypothesis that stage I is the most critical stage in forming fatigue cracks. Furthermore, multiaxial HCF strength is estimated with the stress perpendicular to the critical plane. The maximum normal stress ($\sigma_{n\max}$) relative to the plane with maximum shear stress amplitude (τ_A) is used to evaluate the detrimental effect of non-zero mean normal stress, /48-52/. Therefore, according to the critical plane approach theory, fatigue damage depends on both τ_A and $\sigma_{n\max}$. It was shown that the use of critical distance approach resulted in highly conservative predictions for notches with high stress gradients, /53-54/. The stress gradient is associated with a fairly steep decrease of stress below and also along the surface. For very sharp notches, the elastic stress show singularities /55/. Stress gradient are of paramount importance in notched parts according to Siebel and Stieler /56/, Peterson /57/, Neuber /58/ and others /59-61/. Evidently, fatigue strength depends not only on the value of the elastic stress but also on their spatial distribution, because fatigue at a point is a nonlocal phenomenon, /55/. The surrounding of the continuum contributes to the fatigue. This led to the conception of the "micro-structural support" by Neuber. The lattice structures of materials suggest that the movement of an atom is also influenced by its neighbours, /55/. In lattice dynamics this is described by means of the total potential energy of the system involving all of the atoms.

Due to the high stress concentrations in thread roots, complex nonlinear contact interactions, complex loading combinations, and cyclic material nonlinearity, the stress gradient and critical plane approach based on stresses with multiaxial failure criterion is used for fatigue assessment. The aim of this study is to investigate the influence of different stress gradient methods on bolted joint fatigue behaviour and endurance safety factors under different bolt preload forces and eccentric tensile load ratios with both nonlinear FE and HCF analyses.

MODELLING

The FE model consists of bolt, nut, and two plates, as shown in Fig. 1. As can be seen in the figure, a very detailed FE mesh is created in the thread roots for capturing realistic stress distributions. The mesh is created with solid hexahedral elements (Abaqus C3D8 element). Nonlinear contacts are modelled with sliding contact. The coefficient of friction is set to $\mu = 0.1$. According to VDI 2230 Guidelines /62/, for material combination steel-steel in dry state, $\mu = 0.1$–0.23. The bolted joint consist of M10 bolt, strength grade 10.9 with metric standard thread (pitch according to DIN 13-1 and -28, stress cross section and cross section at minor diameter according to DIN 13-28, and minimum yield point according to DIN EN ISO 898-1). FE model is built with 108332 nodes and 95652 elements. The thread

profile is defined as axi-symmetric because it has been found that the helical effect does not influence the load distribution, /63/. Boundary conditions are defined around the plates with symmetry constraints in XY plane and displacements in YZ direction on the kinematic coupling master nodes are prevented to establish a model without rigid body motion. Kinematic couplings are created in the middle of each plate for applying the eccentric forces and to hold the model. In the bolted joint lifetime, the first load is due to bolt tightening. Bolt preload forces (F_p) are defined according to force at yield point ($F_{0.2}$) for M10 bolt, strength grade 10.9, with value of $F_{0.2}$ = 55000 N, /62/. Applied preload forces are defined as 50, 70 and 90% of $F_{0.2}$, respectively. Abaqus command "Bolt Preload" is used for application of forces on the surface in the middle of the bolt shank. Cyclic eccentric tensile forces (F_e) are defined at 40 mm distance from bolt axis. Maximal and minimal tensile forces are 7000 and 700 N. Load ratio with constant amplitude of 0.1, 0.5, and 0.9 are applied, respectively. V1 represents the fatigue evaluation position at thread roots. Table 1 shows all calculation models with defined bolt preload forces and cyclic load ratios.

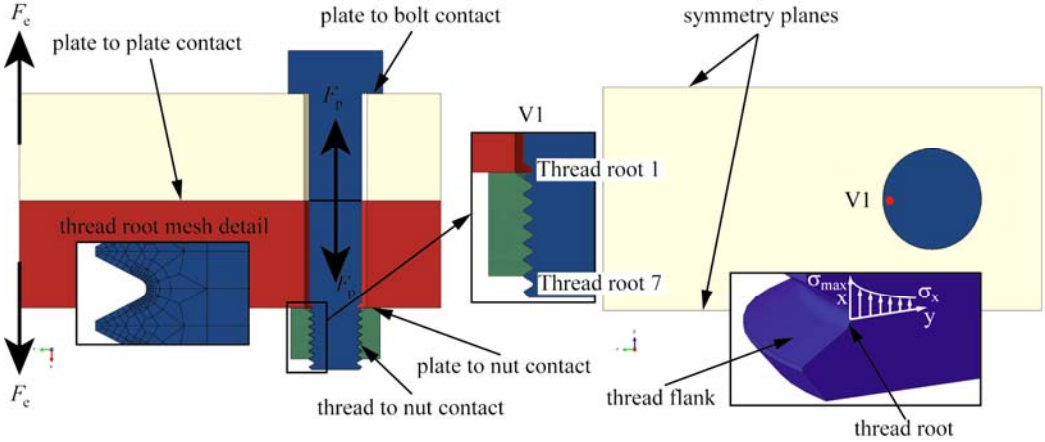

Figure 1. FE model of the bolted joint.
Slika 1. Model konačnih elemenata vijčanog spoja

Numerical analyses are done on FEM model in Abaqus 6.10 (Simulia, Providence, RI, USA). The stress tensors with influence factors and nonlinear cyclic material properties are further calculated in the FemFat 4.8 (ECS, Steyr, Austria) software and endurance safety factors, stress gradient influence factors on fatigue limit and the S-N curve slope are estimated.

MONOTONIC AND CYCLIC MATERIAL PROPERTIES

For bolt strength grade 10.9, the frequently used material is 42CrMo4, /25/. Material monotonic and cyclic properties are shown in Table 1. According to DIN EN 10 083-1 this material is in the class of heat treatable steel, /64/. Cyclic stress-strain hysteresis loop behaviour is defined with cyclic coefficient of hardening $K' = 1.61 \cdot R_m$ and cyclic exponent of hardening $n' = 0.15$, /65, 66/. Table 2 shows the material monotonic and cyclic properties.

Basic cyclic material properties for smooth unnotched circular specimen, S–N curve for alternating tensile/compressive loading (stress ratio $R = -1$) and relative stress gradient $\chi' = 0$ with survival probability defined at 50% is shown in Fig. 2(a). Standard diameter of the specimen is 7.5 mm. The fatigue limit of basic material under alternating stress has a knee-point in the S-N curve at a fatigue life of $2 \cdot 10^6$ cycles and the slope of S-N curve is $k = 12$. Alternating fatigue strength under tension/compression ($R = -1$) was set to $\sigma_{D,tc}$ = 495 MPa, /64/. This material is modified locally at each node of the FE model to obtain correct S–N curve and Haigh diagram at critical areas. The mean stress influence is taken into account by Haigh diagram, which is generated by polygonal lines. Fatigue strength is decreased for tensile mean stress and increased for compressive mean stress. Therefore, the Haigh diagram is unsymmetrical, as shown in Fig. 2(b). Mean stress rearrangement is done according to Neuber-hyperbola with FemFat PLAST.

Table 1. Calculations model.
Tabela 1. Proračunski modeli

Model	% of $F_{0.2}$	Cyclic load ratio
1	50	0.1
2	70	0.1
3	90	0.1
4	50	0.5
5	70	0.5
6	90	0.5
7	50	0.9
8	70	0.9
9	90	0.9

Table 2. Monotonic and cyclic properties for 42CrMo4 steel.
Tabela 2. Monotonička i ciklička svojstva čelika 42CrMo4

Property	Value
Modulus of elasticity, E [MPa]	210000
Poisson coefficient, ν [-]	0.3
Tensile strength, R_m [MPa]	1100
Yield strength, $R_{0.2}$ [MPa]	900
Cyclic coefficient of hardening, K' [MPa]	1771
Cyclic exponent of hardening, n' [-]	0.15
Elongation at fracture, A [%]	11

a)

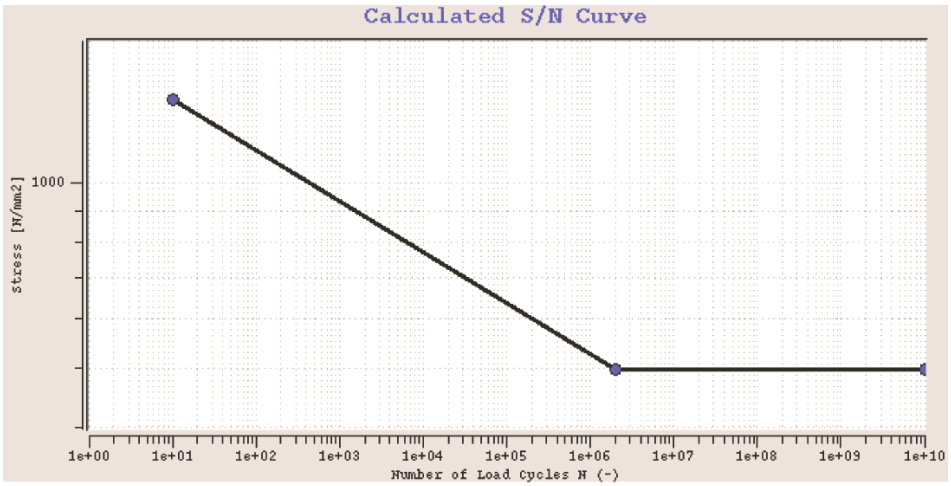

b)

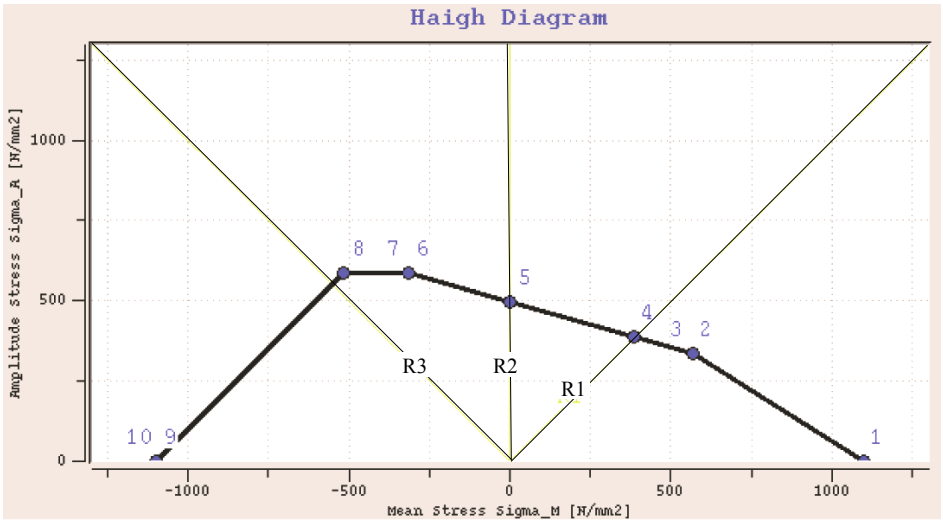

Figure 2. 42CrMo4 steel: (a) S–N curve, and (b) Haigh diagram.
Slika 2. Čelik 42CrMo4: (a) S-N kriva i (b) Hejgov dijagram

MULTIAXIAL HIGH-CYCLE FATIGUE

The calculation of local S-N curve starts with the known basic smooth unnotched specimen S-N curve. At each bolt node the particular local S-N curve is calculated from the specimen cyclic fatigue properties and influencing factors. The definition of the S-N curve model in the double logarithmic system is that the linear damage accumulation is done with the amplitude stress tensor of the particular hysteresis. Other influences like stress distribution, notch effects, size/diameter, mean stress, mean stress rearrangement due to local plastification, surface roughness and statistics (range of dispersion and survival probability) are taken into account at a locally modified S-N curve to obtain correct endurance fatigue limit at critical areas. The multiaxial interaction between stress amplitude tensors and mean stress tensors is solved with critical plane approach in combination with the Haigh diagram. If in the loading spectrum of a bolted structure local stress values are in the elasto-plastic area of the material, then mean stress tensors are rearranged by means of Neuber-hyperbola rule in the cycle stabilised stress-strain curve. The Haigh diagram is used to define the most critical cutting plane angle and the damaging factor for each node. The cutting plane is defined for every 10°. The plane with maximum damage is assumed to be critical for fatigue failure. The relative stress gradient (χ') influences the local S-N curve (both slope k and endurance cycle limit N_e), and endurance stress limit σ_E. Mean stress and surface roughness influence also the local S-N curve, and endurance stress limit σ_E, whereas influence factors as size and statistics influence only endurance stress limit σ_E. Results of safety factors (SF) against endurance limit are for constant stress ratio (R) in the Haigh diagram:

$$SF = \frac{\sigma_{Aall}}{\sigma_A} \tag{1}$$

where σ_{Aall} is the allowable stress amplitude and σ_A is the maximum stress amplitude during fatigue load spectrum.

The Miner linear damage accumulation hypothesis is used for evaluating fatigue life. The equivalent stress algorithm used for multiaxial fatigue failure is a scaled normal stress in critical plane. This algorithm takes the damaging effect of shear into account and is recommended for ductile materials, /67/. From the resulting equivalent stress history, a Rainflow cycle counting is applied to identify closed cycles in the stress-strain path. This means that the resultant loading is saved in a square 64 × 64 amplitude/mean stress matrix. The Rainflow counting method has been shown to

be a superior method compared to peak, range and range-pair, /68/.

The multiaxial fatigue criteria are based on the fatigue crack initiation stage and the fatigue crack growth stage is not included. Micro-crack initiation and initial micro-crack growth are a surface phenomenon, /2/. The surface roughness indicates that stress concentrations along the surface exist due to the rough surface profile. Influence of surface roughness is very significant for HCF, because the fatigue limit of the S-N curve decreases with increasing values of roughness and it also shifts the knee of the S-N curve. The shift of the knee is due to the fact that rougher the surface, the lower the number of cycles to initiate the fatigue crack. The factor is determined using FKM-Guidelines/IABG /64/. The bolt thread surface roughness is defined as R_z = 2.5 μm. Influence of size is also taken into account. Size is defined with a bolt diameter of 10 mm. It has been found that the fatigue life reduces as the bolt nominal size increases /69, 25/. The size influence factor is determined in accordance with FKM-Guidelines, /64/. The range of dispersion (T_S) is defined as the ratio of the bolt fatigue strength at 10% survival probability to fatigue strength at 90% survival probability. The recommended value for steel is 1.26 /67/. Calculations are done with very high survival probability of $P_ü$ = 99.99%. The statistics applied regarding distribution type is the Gaussian Log-Normal distribution for the calculation of statistics influencing variables, both for range of dispersion and survival probability.

High stress gradients resulting from stress concentrations in thread roots by bending of the bolt and thread flanks cause the material surface to be supported with a micro support effect, which results in higher surface fatigue strength. Therefore, fatigue limits under bending conditions are always higher than under the tension/compression. The gradient support effect is confirmed in research with tension/compression and bending fatigue experimental investigations, /70-75/. The basis of stress gradients is verified by many experimental investigations, /76, 77/ and a mathematical model according to /78/ is proposed for the relationship between the support effect and relative stress gradient. The gradient support effect is determined with the relative stress gradient (χ'). In general, with an increase of the notch sharpness, the slope k becomes steeper and the number of cycles at the fatigue limit N_e decreases in S-N curve. The equivalent von Mises stresses σ_e in the nodes are calculated and the average value is formed. Calculation of stress gradient is done for each finite element between neighbouring nodes with the following equation:

$$\chi = \frac{d\sigma_e}{dx} \tag{2}$$

The result of Eq.(2) is the maximum stress gradient $\chi_{\max}$ (regardless of direction) at each node. The relative stress gradient, χ' is determined in FemFat /66/ as:

$$\chi' = \frac{\chi_{\max}}{\sigma_e} \tag{3}$$

Furthermore, support effects are evaluated with the following methods:

1. Stieler,
2. IABG,
3. FemFat and,
4. FKM-Guidelines.

According to Stieler's method and modified by /79/, the support effect factor n is a function of the relative stress gradient (χ') and material yield strength ($R_{p0.2}$):

$$n = 1 + \sqrt{\chi'} \cdot 10^{-\left(0.33 + \frac{R_{p0.2}}{712}\right)} \tag{4}$$

According to the IABG method /80/, the support effect factor for steel is:

$$n = 1 + 0.45 \cdot \chi'^{0.3} \tag{5}$$

This has been calculated for about 600 S-N curves with different notches and statistically evaluated.

According to FemFat method /76, 66/, the ratio of cyclic tensile/compressive strength to the cyclic bending fatigue strength can be used to calculate the support factor n:

$$n = f_{GR,af} = 1 + \frac{(\sigma_{A,b}/\sigma_{A,tsc})}{(2/b)^{\nu}} \chi'^{\nu} \tag{6}$$

where $\sigma_{A,b}$ is the material alternating stress limit for bending and $\sigma_{A,tsc}$ the material alternating stress limit for tension/compression. The material parameter ν takes into consideration the nonproportional increase in the support effect with regard to the relative stress gradient. For steel, ν = 0.3 /66/. Specimen thickness is b. From Eq.(6), in the case of a smooth specimen under bending load with a diameter $d = b$, the factor $f_{GR,af}$ represents the ratio of the cyclic bending fatigue strength to the cyclic tensile/compressive strength (cyclic tensile/compressive strength is multiplied by the factor n to determine the endurance stress limit of the local component S-N curve). Factor $f_{GR,af}$ is the stress gradient factor influencing the fatigue limit.

The influence of the relative stress gradient on the slope $k_{C,GR}$ of the local component S-N curve is calculated with the following equations:

$$f_{GR,sf} = 1 + \frac{1.8\chi'^{1} \cdot 2}{f_{GR,af}} \chi'^{\nu} \tag{7}$$

$$k_{C,GR} = \frac{(k_M - IFK2)}{f_{GR,sf}^{IFK3}} + IFK2 \tag{8}$$

where $f_{GR,sf}$ is the stress gradient influence factor affecting the slope of the local component S-N curve, $k_{C,GR}$ is the slope of the local component S-N curve as a result from the gradient influence, k_M is the slope of the material S-N curve at R = –1, $IFK2$ is the slope exponent of the specimen fracture S-N curve (for the steel, $IFK2$ = 3, /66/), $IFK3$ is the material class dependent exponent (for the steel, $IFK3$ = 2, /66/). The influence of the relative stress gradient on endurance cycle limit $N_{cf,C,GR}$ of the local component S-N curve is calculated with the following equations for steel /80/:

$$N_{cf,C,GR} = N_{cf,M} \cdot f_{GR,cf} \tag{9}$$

$$f_{GR,cf} = \frac{10^{(6.4 - 2.5/k_{c,GR})}}{10^{(6.4 - 2.5/k_M)}} \tag{10}$$

where $N_{cf,C,GR}$ is the endurance cycle limit of local component S-N curve as a result of gradient influence, $N_{cf,M}$ is the endurance cycle limit of material S-N curve at $R = -1$, $f_{GR,cf}$ is the gradient influence factor affecting the endurance cycle limit of the local component S-N curve.

According to FKM-Guidelines /64/, the support factor can be calculated in dependence of relative stress gradient: for $\chi' \leq 0.1$ MPa/mm the support factor n can be calculated:

$$n = 1 + \chi' \cdot 10^{-\left(a_G - 0.5 + \frac{R_m}{b_G}\right)} \quad (11)$$

for 0.1 MPa/mm < $\chi' \leq 1$ MPa/mm the support factor n is:

$$n = 1 + \sqrt{\chi'} \cdot 10^{-\left(a_G + \frac{R_m}{b_G}\right)} \quad (12)$$

for 1 MPa/mm < $\chi' \leq 100$ MPa/mm the support factor n is:

$$n = 1 + \sqrt[4]{\chi'} \cdot 10^{-\left(a_G + \frac{R_m}{b_G}\right)} \quad (13)$$

where a_G and b_G are constants and for the steel materials are 0.5 and 2700, respectively, /64/.

RESULTS AND DISCUSSION

The fatigue assessments are carried out with the following methods: FemFat, FKM, IABG, and Stieler, for taking stress gradient influence into account and as well as without influence of the stress gradients. The first step was defined as bolt tightening. Maximal principal stress distribution after tightening with 50% of $F_{0.2}$ can be seen in Fig. 3a. Furthermore, maximal principal stress distribution after the maximum eccentric tensile forces which induce the bending loads on the bolt is shown in Fig. 3b. Deformation scale in the figures is set to 25. The bolt preload force is activated in all further steps to achieve bolted joint in preloaded condition. Maximum value of stress is on the first thread root. High value of stresses are present in the model due to linear elastic material properties in the FE analyses. This is the obvious reason to use Neuber-hyperbola for accurate stress distribution and to achieve realistic elastic-plastic behaviour. Highest stress concentrations occur at the first three thread roots due to preload and eccentric tensile forces. As can be seen from these figures, at the bolt head to shank transition radius, stress concentration also occurs. However, at this position, fatigue assessment is not performed.

Fatigue results on bolt shank and thread roots for multiaxial HCF criteria under bolt tightening and cyclic eccentric tensile forces are: relative stress gradients (χ'), endurance safety factors (SF), stress gradient influence on both fatigue limit ($f_{GR,af}$) and slope of the local component S-N curve ($f_{GR,sf}$), respectively. The relative stress gradient distribution in the thread roots reveals that after first engaged thread (thread root 2) gradients increase, as can be observed from Fig. 4a. The increase can be observed from thread root 2 with maximal value of $\chi' = 9$ MPa/mm to $\chi' \approx 20$ MPa/mm at thread root 7. Results show that with the increase of bolt preload force, the stress gradients slightly increase, as can be seen for the first engaged thread in Fig. 4b.

The assessment with the IABG method provides the highest stress gradient influence factors on fatigue limit, whereas the Stieler method provides the lowest factors. Correlation of stress gradient influence factors on fatigue limit for all methods and models are presented in Fig. 5a–j. As can be seen from these figures, regardless of the bolt preload forces and stress ratios used for obtaining factors, the results are similar. The only significant difference is between used methods. With IABG method at first engaged thread, $f_{GR,af} = 1.9$. Further thread roots (from thread root 2 to 7) show slightly higher values of influence factors. On models 2, 3, and 6, small peaks can be observed.

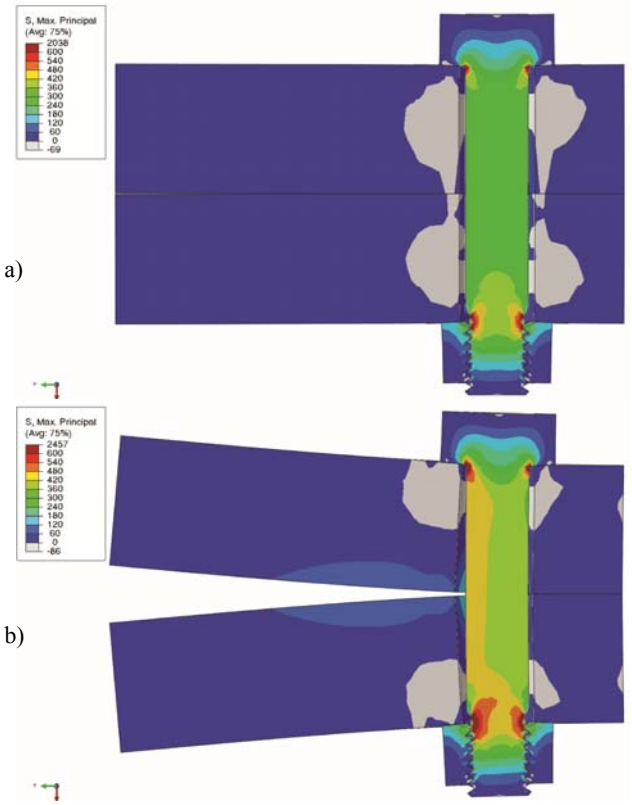

Figure 3. Maximal principal stress distribution in bolted joint (a), due to preload force; (b) due to preload force and maximal tensile eccentric force.

Slika 3. Raspodela glavnih napona u vijčanom spoju (a) usled sile pritezanja; (b) usled sile pritezanja i maksimalne zatezne ekscentrične sile

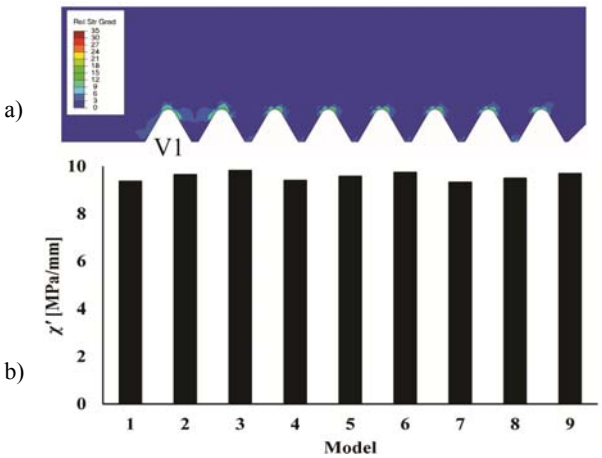

Figure 4. Relative stress gradients (a) distribution in thread roots and (b) comparison between all 9 models.

Slika 4. Relativni gradijenti napona (a) raspodela u korenima navoja i (b) poređenje svih 9 modela

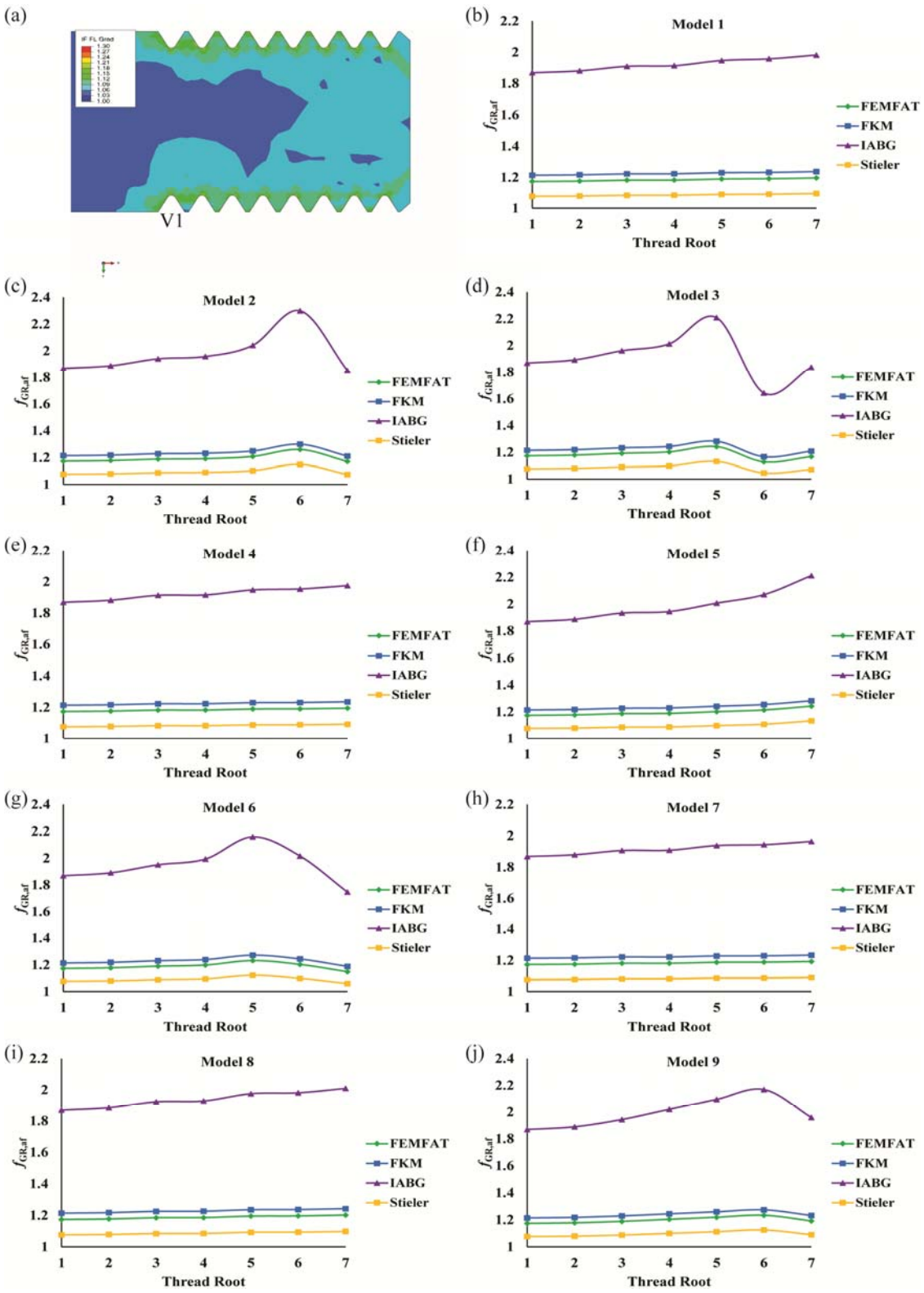

Figure 5. Stress gradient factor influencing the fatigue limit (a) distribution in thread roots; (b) to (j) values for model 1 up to 9.
Slika 5. Uticajni faktori gradijenata napona na dinamičku izdržljivost (a) raspodela u korenu navoja; (b) do (j) vrednosti za modele 1 do 9

However, results for stress gradient influence factors affecting the slope of local component S-N curve are in contrary with stress gradient influence on fatigue limit because assessment with IABG method provides lowest factors, whereas Stieler method provides the highest factors, as shown in Fig. 6a–j. As can be seen from these figures, this factor at first engaging the thread root with the Stieler method is $f_{GR,sf} = 30$ in Model 3. Similar to stress gradient influence factors on fatigue limit, the obtained influence factors on slope are similar in all 9 models regardless of bolt preload forces and stress ratios. As can be seen from these figures, only significant difference is again between used methods.

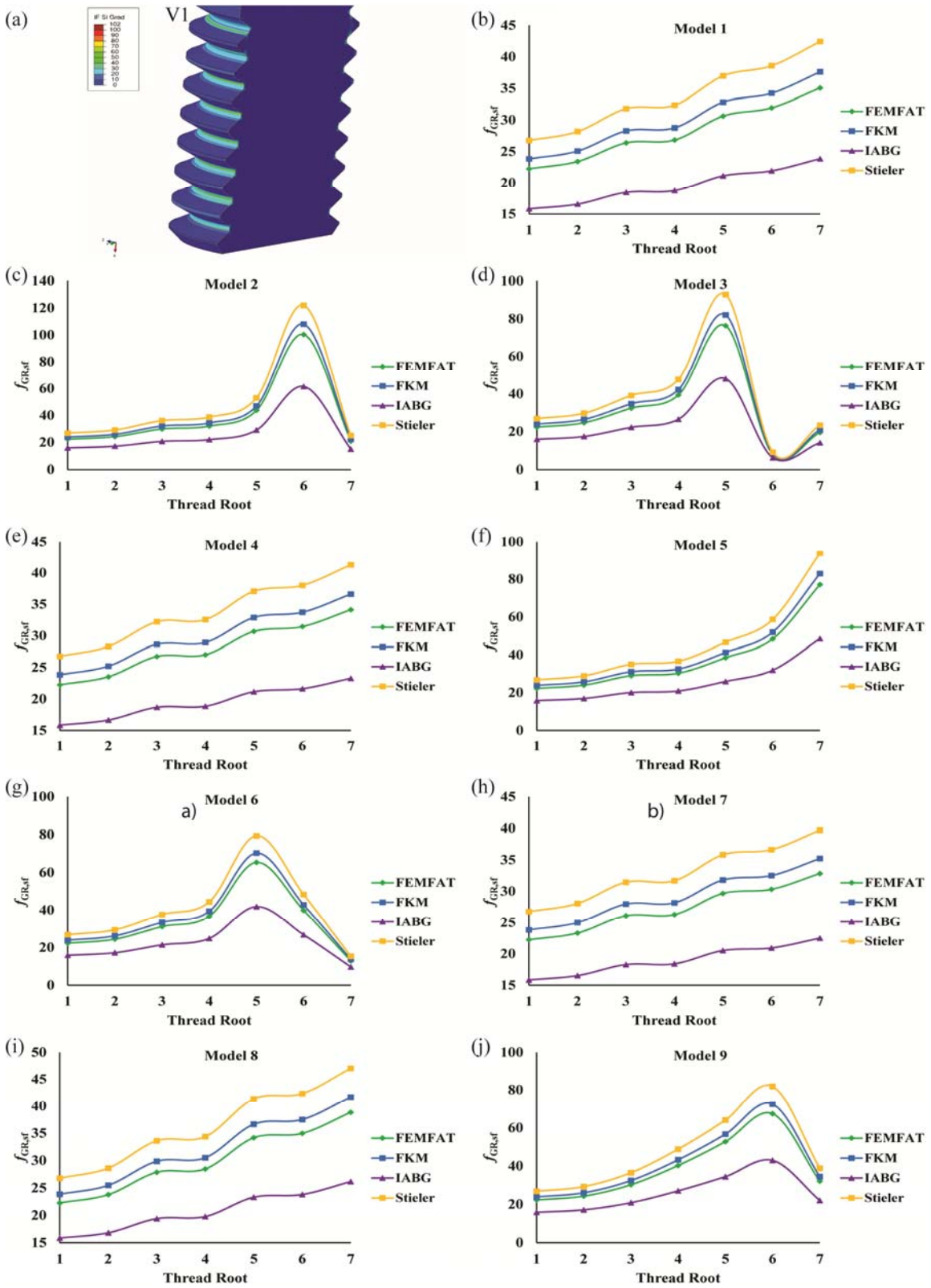

Figure 6. Stress gradient factor influencing the slope of the local component S-N curve, (a) distribution in thread roots; (b)-(j) values for models 1 up to 9.

Slika 6. Uticajni faktori gradijenata napona na nagib lokalne S-N krive, (a) raspodela u korenu navoja; (b)-(j) vrednosti za modele 1 do 9

The fatigue assessment of the endurance safety factors (SF) shows that the minimal SF regardless of the bolt preload and stress ratio is always on the first engaged thread root, as can be observed from Fig. 7a–j. The method without the influence of stress gradients results with minimal SF = 0.77 in Model 1. The assessment with methods which takes the influence of stress gradients into account, result with minimal SF = 0.81. Minimal SF are obtained using

Stieler method because stress gradient factors influencing the fatigue limit are lowest, as is previously shown in Fig. 5a–j. The assessment with the IABG method provides the highest stress gradient influence factors on fatigue limit which in turn result with maximal SF = 1.14, at first engaged thread root. FemFat and FKM methods have obtained very similar minimal SF ≈ 0.87. Thread roots after first engaged thread have higher SF. It is interesting to observe from Fig. 7b–j that SF at thread run-out (i.e., thread root 1) have lower SF than at thread root 2 and further.

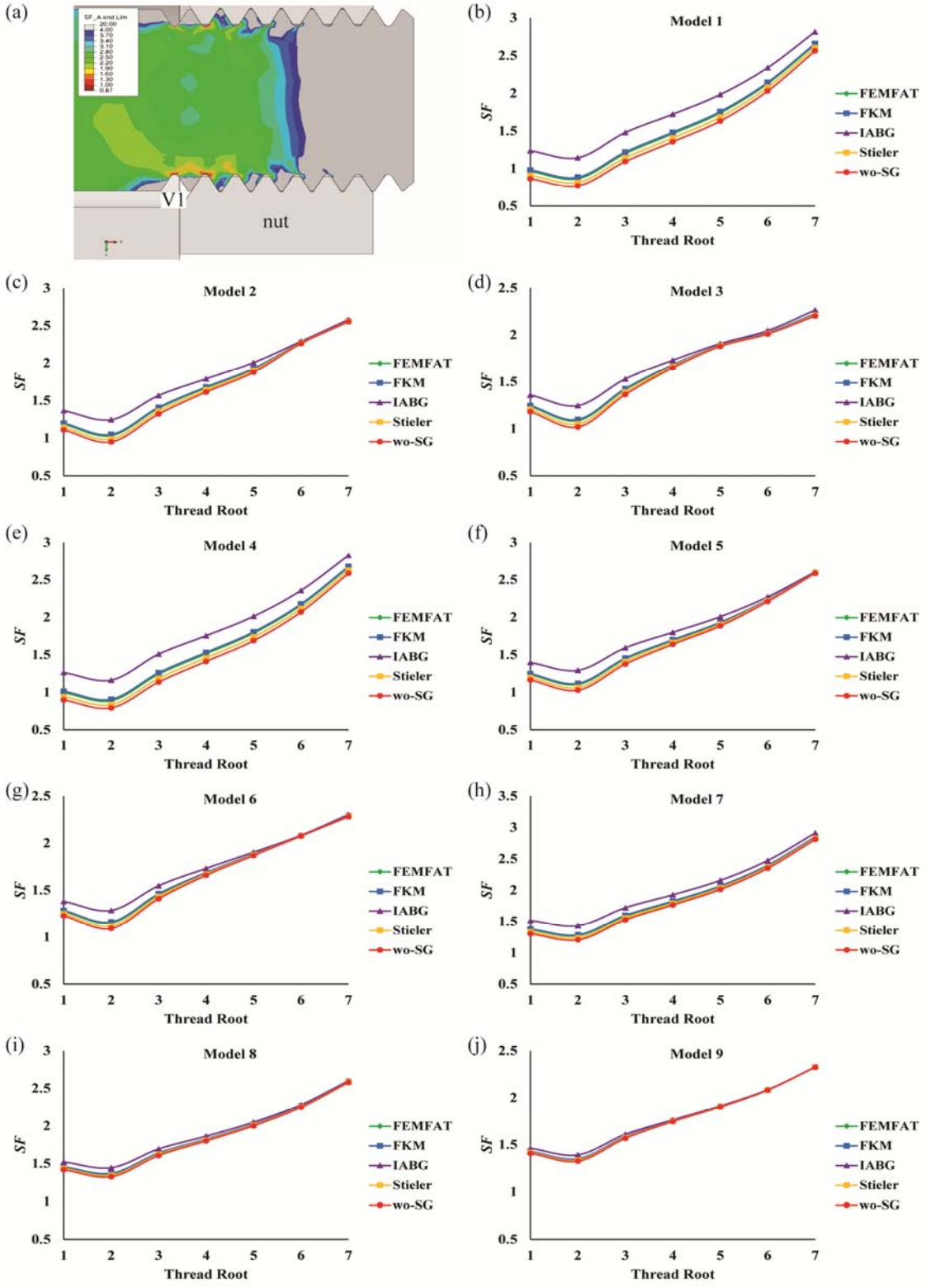

Figure 7. Endurance *SF* (a) distribution in thread roots, and from (b) to (j) values at thread roots for models 1 up to 9, respectively.
Slika 7. Faktori sigurnosti dinamičke izdržljivosti (a) raspodela u korenima navoja, i od (b) do (j) vrednosti za modele od 1 do 9

The obtained relative stress gradients at bolt shank show very low values, as can be observed from Fig. 8. Similar as for the thread roots, stress gradients at bolt shank slightly increase due to increase of the bolt preload force. Maximal $\chi' = 0.09$ MPa/mm at bolt shank in Model 3 is obtained. In comparison with relative stress gradients at thread roots, values at bolt shank are incomparably lower. The bolt shank is a smooth cylindrical body without notches which contains significant preload force and therefore, in this case significant stress gradients do not occur.

The assessment of stress gradient influence on fatigue limit for bolt shank with IABG method provides the highest influence factors, whereas the Stieler method provides the lowest factors, as shown in Fig. 9. As can be seen from this figure, regardless of the bolt preload force and stress ratio used for obtaining factors, the results are similar. Only significant difference is between used methods. With IABG method at bolt shank, $f_{GR,af} = 1.21$ in Model 3.

The assessment of stress gradient influence factors affecting the slope of local component S-N curve with Stieler method provides the highest factors, as shown in Fig. 10. As can be seen from this figure, regardless of the bolt preload force and stress ratio used for obtaining factors, the results are similar. Only significant difference is between used methods. With Stieler method at bolt shank, $f_{GR,sf} = 1.1$ in Model 3.

Fatigue assessment of the endurance safety factors at bolt shank shows that the minimal SF = 1.91 is obtained without the influence of stress gradients in Model 3, as can be observed from Fig. 11. FemFat, FKM and Stieler method obtained with very similar SF values. IABG method obtained maximum safety factor, SF = 1.93. With the IABG method, highest stress gradient influence factors on fatigue limit are obtained, which in turn provide significantly higher safety factors. As can be seen in Fig. 11, it is interesting to observe that safety factors at bolt shank decrease with the increase of bolt preload, as opposite to thread roots, where safety factors simultaneously increase with the bolt preload force.

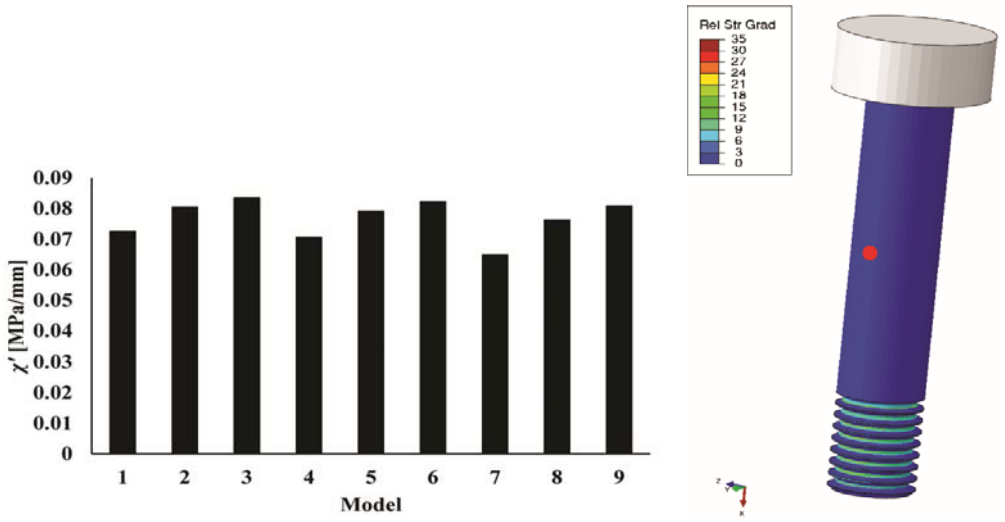

Figure 8. The relative stress gradients obtained at bolt shank.
Slika 8. Relativni gradijenti napona na telu vijka

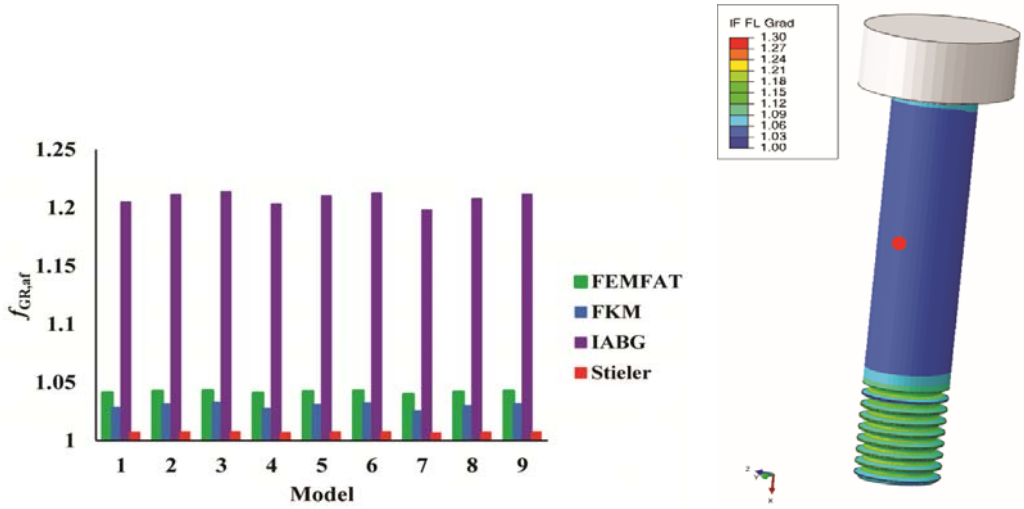

Figure 9. The stress gradient influence factors on fatigue limit at bolt shank.
Slika 9. Uticajni faktori gradijenata napona na dinamičku izdržljivost na telu vijka

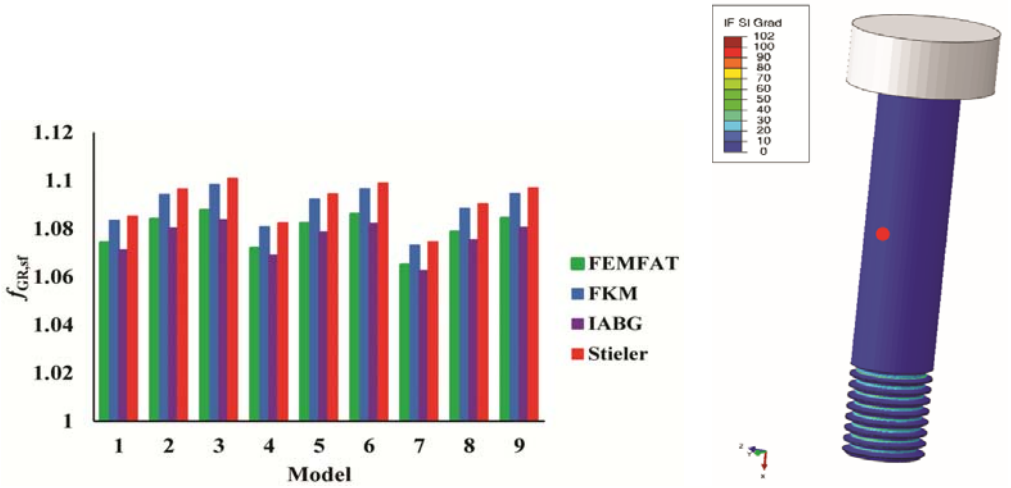

Figure 10. The stress gradient influence factors affecting the slope of the local component S-N curve at bolt shank.
Slika 10. Uticajni faktori gradijenata napona na nagib S-N krive na telu vijka

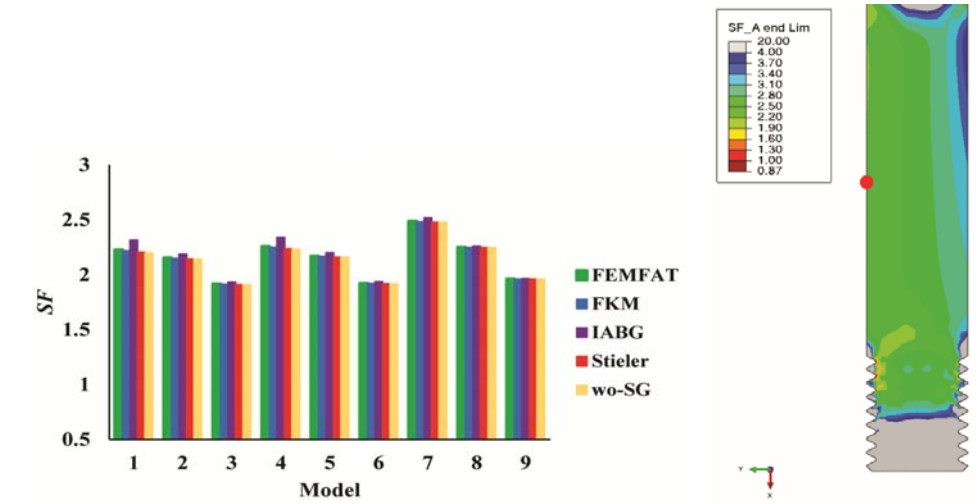

Figure 11. Endurance safety factors at bolt shank.
Slika 11. Faktori sigurnosti dinamičke izdržljivost na telu vijka

As can be seen, all methods for taking stress gradient influence into account provide the higher endurance safety factors. Moreover, it can be observed that stress gradients in thread roots have beneficial influence on fatigue behaviour. However, the bolt shank stress gradients do not have significant influence. Stress gradients allow to describe complete stress field at thread roots. Nevertheless, as mentioned earlier, in all models the highest stress concentration factor and minimal SF is in the first engaged thread root. These results, based on critical plane approach with taking into account complete stress field at the thread root with gradient dependent multiaxial fatigue methods, are in accordance with previous investigations which show that fatigue failure occurs in the first engaging thread /3, 69, 81, 82/. Moreover, this approach is also in accordance with studies that show microstructural support effect for fatigue crack initiation at the notch root /59, 60, 61, 70-78/. Notches reduce the fatigue strength and life significantly, but not to the extent of the elastic stress concentration /59/. Furthermore, it is found that eccentric loading does not affect the shape of fatigue cracks significantly, /31/. Moreover, as previously mentioned, the use of critical distance approach resulted with highly conservative results for notches with high stress gradients, /53-54/, the stress gradient and critical plane approach based on stresses with fatigue influence factors can take realistic stress field at notches into account and in turn obtain more realistic fatigue behaviour assessment.

CONCLUSIONS

The important conclusion to be drawn here are that the obtained endurance safety factors with methods that take the influence of stress gradient into account show higher safety against fatigue failure. The FE and HCF analyses carried out in this work have proven that the significant stress gradients exist and influence the fatigue behaviour of threaded joints. This confirms the correctness of the beneficial stress gradient support effect at thread roots due to the bending of thread flanks. Fatigue assessment of threaded joints without the influence of stress gradients can provide conservative results. The obtained values of endurance safety factors highlight the significant influence of the stress gradient influence on both fatigue limit and slope of the local component S-N curve. The practical application of

stress gradient influence on threaded joint fatigue behaviour requires consideration of used material. This can be described with material parameters that take into account the nonproportional increase in the support effect with regard to the relative stress gradient. Stieler method takes into account the support factor only in dependence from relative stress gradient and yield strength. FemFat, IABG and FKM methods take into account the support factor in addition from dependence of material class due to different notch sensitivity (e.g., for structural heat treatable spring steel, austenitic stainless steel, etc).

The IABG method obtained the highest endurance safety factors due to the highest influence stress gradient factors on fatigue limit. The Stieler method obtained the lowest endurance safety factors. However, the Stieler method obtained the highest stress gradient influence factors affecting the slope of the local component S-N curve.

Slight increase of stress gradients was observed due to the higher bolt preload forces. Stress gradients at bolt shank are incomparably lower than in the thread roots.

Relative stress gradients have slightly higher values after the first engaged thread. But nevertheless, it shows that with the increase of the χ', the support factor also increase. It also gives useful information that apart from the uneven load distribution, a slightly higher support factor is evident from the first engaged thread.

ACKNOWLEDGEMENTS

The authors would like to thank AVL company for usage of Abaqus and FemFat software.

REFERENCES

1. Schijve, J., *Fatigue of Structures and Materials in the 20th Century and the State of the Art*, Int. J Fatigue, 25 (2003), pp.679-702.
2. Schijve, J., *The significance of fatigue crack initiation for predictions of the fatigue limit of specimens and structures*, Int. J Fatigue, 61 (2014), pp.39-45.
3. Cho, S.S., Chang, H., Lee, K.W., *Dependence of fatigue limit of high-tension bolts on mean stress and ultimate tensile strength*, Int. J Automot. Techn., Vol.10, No.4 (2009), pp.475-479.
4. Esaklul, K.A., Ahmed, T.M., *Prevention of failures of high strength fasteners in use in offshore and subsea applications*, Eng. Fail. Anal., 16 (2009), pp.1195-1202.
5. Sungkon, H., *Fatigue Analysis of Drillstring Threaded Connections*, Proc. of The Thirteenth (2003) International Offshore and Polar Engng. Conf. Honolulu, Hawaii, USA, May 25-30, 2003, The Intern. Soc. of Offshore and Polar Engineers, pp.202-208.
6. Shahani, A.R., Sharifi, S.M.H., *Contact stress analysis and calculation of stress concentration factors at the tool joint of a drill pipe*, Mater. Des., 30 (2009), pp.3615-3621.
7. Den Hartog, J.P., *The mechanics of plate rotors for turbo generators*, Am. Soc. Mech. Eng. Trans. Appl. Mech. (1929), 51 (10), pp.1-9.
8. Dragoni, E., *Effect of nut geometries on screw thread stress distribution, Photoelastic results*, J Strain Anal. Eng. Des. (1992), 27 (1), pp.1-6.
9. Goodier, J.N., *The distribution of load on the threads of screws*, J Appl. Mech., 7 (1940), A10–A16.
10. Kenny, B., Patterson, E.A., Load and stress distribution in screw threads. Exp. Mech. (1985), 25 (3), pp.208-213.
11. Patterson, E.A., Kenny, B., *A modification to the theory for the load distribution in conventional nuts and bolts*, J Strain Anal. Eng. Des. (1986), 21 (1), pp.17-23.
12. Sopwith, D.G., *The distribution of load in screw threads*, Inst. Mech. Eng. Proc. (1948), 159 (45), pp.373-383.
13. Surtees, J.O., Nip, T.F., *Use of threaded rod compression stiffening in end plate connections*, Struct. Eng. (2001), 79 (11), pp.22-27.
14. D'Eramo, M., Cappa, P., *An experimental validation of load distribution in screw threads*, Exp. Mech. (1991), 31 (1), pp.70-75.
15. Bretl, J.L., Cook, R.D., *Modelling the load transfer in threaded connections by the finite element method*, Int. J Numer. Meth. Eng. (1979), 14 (9), pp.1359-77.
16. Izumi, S., Yokoyama, T., Iwasaki, A., *Three-dimensional finite element analysis of tightening and loosening mechanism of threaded fastener*. Eng. Fail. Anal (2005), 12 (4), pp.604-615.
17. Vahid-Araghi, O., Golnaraghi, F., *Friction-induced vibration in lead screw drives*, 1st Ed. New York: Springer; 2011. pp.67-84.
18. Lu, S., Han, Y., Qin, T.C., *Analysis of well casing connection pullout*, Eng. Fail. Anal. (2006),13 (4), pp.638-45.
19. Lo Conte, A., Cucchetti, F., Marangoni, M., *Experimental and numerical study of expandable threaded connections and proposal of a new design*, Int. J Mater. Prod. Technol. (2007), 30 (1-3), pp.216-242.
20. Kenny, B., Patterson, E., *Load and stress distribution in screw threads*, Exp. Mech. (1985), 25 (3), pp.208-213.
21. Wang, W., Marshek, K.M., *Determination of load distribution in a threaded connector with yielding threads*, Mech. Mach. Theory (1996), 31 (2), pp.229-244.
22. Wang, W., Marshek, K.M., *Determination of the load distribution in a threaded connector having dissimilar materials and varying thread stiffness*, J Eng. Ind. (1995), 117(1), pp.1-8.
23. Chen, S.-J., Zhang, Y., Gao, L.-X., Li, Q., An, Q., *Loading analysis on the thread teeth in cylindrical pipe thread connection*, J Press. Ves. Technol. (2010), 132 (3), pp.031202-031208.
24. Dragoni, E., *Effect of nut geometries on screw thread stress distribution: photoelastic results*, J Strain Anal. Eng. Des. (1992), 27 (1), pp.1-6.
25. Wiegand, H., Kloos, K.-H., Thomala, W., Schraubenverbindungen: Grundlagen, Berechnung, Eigenschaften, Handhabung, 5. Auflage, Springer-Verlag Berlin, 2007.
26. Schneider, R., Wuttke, U., Berger, C., *Fatigue Analysis of Threaded Connections Using the Local Strain Approach*, Procedia Engineering (2010), 2 (1), pp.2357-2366.
27. Ferjani, M., Averbuch, D., Constantinescu, A., *A computational approach for the fatigue design of threaded connections*. Int. J Fatigue, 33 (2011), pp.610-623.
28. Fares, Y., Chaussumier, M., Daidie, A., Guillot, J., *Determining the life cycle of bolts using a local approach and the Dang Van criterion*, Fatigue Fract. Eng. Mater. Struct., 29 (2006), pp.588-596.
29. Hofmann, F., Bertolino, G., Constantinescu, A., Ferjani, M., *A multiscale discussion of fatigue and shakedown for notched structures*. Theor. Appl. Fract. Mech. (2007), 48(2), pp.140-151.
30. Hofmann, F., Bertolino, G., Constantinescu, A., Ferjani, M., *A discussion at the mesoscopic scale of the stress-gradient effects in high cycle fatigue based on the Dang Van criterion*, J Mech. Mater. Struct. (2009), 4 (2), pp.293-308.

31. Hobbs, J.W., Burguete, R.L., Heyes, P.F., Patterson, E.A., *The effect of eccentric loading on the fatigue performance of high-tensile bolts*, Int. J Fatigue, 22 (2000), pp.531-538.
32. Patterson, E.A., *A comparative study of methods for estimating bolt fatigue limits*, Fatigue Fract. Eng. Mater. Struct. (1990), 13 (1), pp.59-81.
33. Fares, Y., Chaussumier, M., Daidie, A., Guillot, J., *Determining the life cycle of bolts using a local approach and the Dang Van criterion*, Fatigue Fract. Engng. Mater. Struct., 29 (2006), pp.588-596.
34. Liao, R., Sun, Y., Liu, J., Zhang, W., *Applicability of Damage Models for Failure Analysis of Threaded Bolts*, Engineering Frac. Mech. (2011), 78 (3), pp.514-524.
35. Naik, R.A., Lanning, D.B., Nicholas, T., Kallmeyer, A.R., *A critical plane gradient approach for the prediction of notched HCF life*, Int. J Fatigue, 27 (2005), pp.481-492.
36. Karolczuk, A., Macha, E., *A review of critical plane orientations in multiaxial fatigue failure criteria of metallic materials*, Int. J of Fracture, 134 (2005), pp.267-304.
37. Findley, W.N., *A theory for effect of mean stress on fatigue of metals under combined torsion and axial load or bending*, J Eng. Ind. (1959), pp.301-306.
38. Forsyth, P.J.E., *A two stage process of fatigue crack growth*, McDowell DL, editor, Proceedings of the Crack Propagation Symposium, Cranfield, 1961, pp.76-94.
39. Jahed, H., Varvani-Farahani, A., *Upper and lower fatigue life limits model using energy-based fatigue properties*, Int. J Fatigue, 28 (2006), pp.467-473.
40. McDiarmid, D.L., Failure criteria and cumulative damage in fatigue under multiaxial stress conditions, PhD Dissertation, Department of Mechanical Engineering, The City University of London, 1972.
41. Susmel, L., Tovo, R., *Estimating fatigue damage under variable amplitude multiaxial fatigue loading*, Fatigue Fract. Engng. Mater. Struct., 34 (2011), pp.1053-1077.
42. Łagoda, T., Macha, E., *Estimated and experimental fatigue lives of 30CrNiMo8 steel under in-and out-of-phase combined bending and torsion with variable amplitude*, Fatigue Fract. Eng. Mat. Struct., 11 (1994), pp.1307-1318.
43. Morel, F., *A critical plane approach for life prediction of high cycle fatigue under multiaxial variable amplitude loading*, Int. J Fatigue, 22 (2000), pp.101-119.
44. Carpinteri, A., Spagnoli, A., Vantadori, S., *A multiaxial fatigue criterion for random loading*, Fatigue Fract. Eng. Mat. Struct., 26 (2003), pp.515-522.
45. Łagoda, T., Ogonowski, P., *Criteria of multiaxial random fatigue based on stress, strain and energy parameters of damage in the critical plane*. Mat.-wiss. u. Werkstofftech., 36 (2005), pp.429-437.
46. Marciniak, Z., Rozumek, D., Macha, E., *Fatigue lives of 18G2A and 10HNAP steels under variable amplitude and random non-proportional bending with torsion*. Int. J Fatigue, 30 (2008), pp.800-813.
47. Karolczuk, A., Macha, E., *Selection of the critical plane orientation in two-parameter multiaxial fatigue failure criterion under combined bending and torsion*, Engineering Fracture Mechanics, 75 (2008), pp.389-403.
48. Matake, T., *An explanation on fatigue limit under combined stress*, Bull. JSME, 20 (1977), pp.257-263.
49. McDiarmid D.L., *A shear stress based critical-plane criterion of multiaxial fatigue failure for design and life prediction*, Fatigue Fract. Eng. Mater. Struct., 17 (1994), pp.1475-1484.
50. Susmel, L., Lazzarin, P., *A bi-parametric modified Wöhler curve for high cycle multiaxial fatigue assessment*, Fatigue Fract. Eng. Mater. Struct., 25 (2002), pp. 63-78.
51. Susmel, L., Petrone, N., *Multiaxial fatigue life estimations for 6082-T6 cylindrical specimens under in-phase and out-of-phase biaxial loadings*, Biaxial and Multiaxial Fatigue and Fracture, (Eds. A. Carpinteri, M. de Freitas, and A. Spagnoli), Elsevier and ESIS, Oxford, UK, 2003, pp. 83-104.
52. Lazzarin, P., Susmel, L., *A stress-based method to predict lifetime under multiaxial fatigue loadings*, Fatigue Fract. Eng. Mater. Struct., 26 (2003), pp.1171-1187.
53. Bellett, D., Taylor, D., Marco, S., Mazzeo, E., Guillois, J., Pircher, T., *The fatigue behaviour of three-dimensional stress concentrations*, Int. J Fatigue, 27 (2005), pp.207-221.
54. Bellett, D., Taylor, D., *The effect of crack shape on the fatigue limit of three-dimensional stress concentrations*, Int. J Fatigue, 28 (2006), pp.114-123.
55. Zhang, G., *Method of effective stress for fatigue: Part I - A general theory*, Int. J Fatigue, 37 (2012), pp.17-23.
56. Siebel, E., Stieler, M., *Ungleichformige Spannungsverteilung bei schwingender Beanspruchung (Nonuniform stress distributions under cyclic loading)*. VDI-Z, 97(5) 1955, pp.121-126.
57. Peterson, R.E., *Notch sensitivity*, G Sines, J Waisman, eds. Metal Fatigue, McGraw Hill, New York, 1959, pp.293-306.
58. Neuber, H., *Über die Berücksichtigung der Spannungskonzentration bei Festigkeitsberechnungen (About the consideration of stress concentration in the calculation of strength)*, Konstruktion, 20 (7), 1968, pp.245-251.
59. Radaj, D., Lazzarin, P., Berto, F., *Generalised Neuber concept of fictitious notch rounding*, Int. J Fatigue, 51 (2013), pp.105-115.
60. Berto, F., *Fictitious notch rounding concept applied to V-notches with end holes under mode 3 loading*, Int. J Fatigue, 38 (2012), pp.188-193.
61. Berto, F., Lazzarin, P., Radaj, D., *Fictitious notch rounding concept applied to sharp V-notches: Evaluation of the microstructural support factor for different failure hypotheses. Part I: Basic stress equations*, Engineering Fracture Mechanics, 75 (2008), pp.3060-3072.
62. Verein Deutscher Ingenieure. VDI 2230 Guidelines. 2003.
63. Chen, J.-J., Shih, Y.-S., *A study of the helical effect on the thread connection by three dimensional finite element analysis*, Nuclear Engineering and Design, 191 (1999), pp.109-116.
64. Forschungskuratorium Maschinenbau (FKM), Analytical strength assessment of components in mechanical engineering, 5th Ed. VDMA Verlag GmbH, 2003.
65. Haibach, E., *Betriebsfestigkeit: Verfahren und Daten zur Bauteilberechnung*. 3rd Ed. Berlin: Springer-Verlag; 2006. pp.348
66. ECS Steyr. FemFat 4.7: Theory Manual. St. Valentin, 2007.
67. ECS Steyr. FemFat 4.8: MAX Manual. St. Valentin, 2007.
68. Dowling, N., *Fatigue Failure Predictions for Complicated Stress–Strain Histories*, J of Materials (1972), 7(1):71-78.
69. Majzoobi, G.H., Farrahi, G.H., Habibi, N., *Experimental evaluation of the effect of thread pitch on fatigue life of bolts*, Int. J Fatigue, 27 (2005), pp.189-196.
70. Papadopoulos, I.V., Panoskaltsis, V.P., *Invariant formulation of a gradient dependent multiaxial high-cycle fatigue criterion*, Eng. Fract. Mech. (1996), 55(4):513-528.
71. Moore, H.F., Morkovin, D., *Progress report on the effect of size of specimen on fatigue strength of three types of steel*, Proc. ASTM, 42 (1942), pp.145-153.
72. Moore, H.F., Morkovin, D., *Second progress report on the effect of size of specimen on fatigue strength of three types of steel*, Proc. ASTM, 43 (1943), pp.109-120.
73. Moore, H.F., Morkovin, D., *Third progress report on the effect of size of specimen on fatigue strength of three types of steel*, Proc. ASTM, 44 (1944), pp.137-158.

74. Moore, H.F., *A study of size effect and notch sensitivity in fatigue tests of steel*, Proc ASTM 1945;45:507-31.
75. Morel, F., Morel, A., Nadot, Y., *Comparison between defects and micro-notches in multiaxial fatigue – The size effect and the gradient effect*, Int. J Fatigue (2009), 31(2):263-275.
76. Eichlseder, W., Dissertation, TU Graz, Rechnerische Lebensdaueranalyse von Nutzfahrzeugkomponenten mit der FE-methode, 1989.
77. Eichlseder, W., Unger, B., *Prediction of the Fatigue Life with the Finite Element Method*, SAE Paper 940245.
78. Eichlseder, W., *Fatigue analysis by local stress concept based on finite element results*, Comput. Struct. (2002), 80(27):2109-2113.
79. GDR Standard. TGL 19340: Dauerfestigkeit der Maschinenbauteile, Berlin: GDR State Publisher, 1983.
80. Hück, M., Thrainer, L., Schütz, W., Berechnung von Wöhlerlinien für Bauteile aus Stahl, Stahlguss und Grauguss – Synthetische Wöhlerlinien – Verein deutscher Eisenhüttenleute, Report no. ABF 11, Düsseldorf, 1983.
81. Berger, C., Pyttel, B., Trossmann, T., *Very high cycle fatigue tests with smooth and notched specimens and screws made of light metal alloys*, Int. J Fatigue, 28 (2006), pp.1640-1646.
82. Horn, N.J., Stephens, R.I., *Influence of Cold Rolling Threads Before or After Heat Treatment on High Strength Bolts for Different Fatigue Preload Conditions*. Journal of ASTM International, 2006, Vol.3, No.1, pp.95-115.

Event	Date	Location	Contact
2014			
Residual Stress: Contour Method	2 June	t/b/a	www.fesi.org.uk
OMAE2014 – 33rd International Conference on Ocean, Offshore and Arctic Engineering	8-13 June	San Francisco, California, USA	www.asmeconferences.org
ECF20 – 20th European Conference on Fracture	30 June – 4 July	Trondheim, Norway	www.ecf20.no
ICEFA VI – Sixth International Conference on Engineering Failure Analysis	6-9 July	Lisbon, Portugal	www.icefaconference.com
ASME 2014 Pressure Vessels & Piping Division Conference	20-24 July	Anaheim, California, USA	www.asmeconferences.org
WCCM XI – ECCM V – ECFD VI	20-25 July	Barcelona, Spain	www.wccm-eccm-ecfd2014.org
FEDSM2014 – 4th Joint US-European Fluids Engineering Summer Meeting	3-7 August	Chicago, Illinois, USA	www.calender.asme.org
ICOTOM17 – 17th International Conference on Textures of Materials	24 29 August	Dresden, Germany	http://icotom17.com
CIEC14 – 14th Inter-regional Conference on Ceramics	8-10 September	Stuttgart, Germany	www.ciec14.org
Multi-Lateral Workshop on Fracture and Structural Integrity-related Issues	15-17 September	Catania, Italy	www.gruppofrattura.it
Rolling Bearing Fatigue	t/b/a	Warrington	www.fesi.org.uk
International Conference on Fatigue Damage of Structural Materials X	21-26 September	Hyannis, Maryland, USA	www.fatiguedamageconference.com
IPC 2014 – 10th International Pipeline Conference	28 September - 3 October	Calgary, Alberta, Canada	www.asmeconferences.org
Hydrogen Embrittlement – Multi-scale Modelling and Measurement. What is the Impact?	6-8 October	NPL, Teddington	alan.turnbull@npl.co.uk
SI of Components for Renewable Energy Systems	t/b/a	t/b/a	www.fesi.org.uk
Monitoring and RBI of Offshore Structures	t/b/a	t/b/a	www.fesi.org.uk
2015			
SMiRT 23 – 23rd Conference on Structural Mechanics in Reactor Technology International	10-14 August	Manchester	www.smirt23.org
CP 2015 – 5th International Conference on Crack Paths	16-18 September	Ferrara, Italy	www.structuralintegrity.eu
2016			
ECF21 – 21st European Conference on Fracture	19-24 June	Catania, Italy	www.structuralintegrity.eu
2017			
ICF14 – Fourteenth International Conference on Fracture	7-13 May	Rhodes, Greece	www.icfweb.org